Seventh International Conference on CFD in the Minerals and Process Industries
CSIRO, Melbourne, Australia
9-11 December 2009

CFD-DEM MODELLING OF GAS FLUIDIZATION OF PARTICLE MIXTURES WITH SIZE AND DENSITY DIFFERENCES

Yuqing FENG[1*] and Aibing YU [2]

[1] CSIRO Minerals, Clayton, Victoria 3169, AUSTRALIA

[2] Lab for Simulation and Modelling of Particulate Systems, School of Materials Science and Engineering, The University of New South Wales, Sydney, NSW 2052, AUSTRALIA

* Corresponding author, Yuqing.Feng@csiro.au

ABSTRACT

Mixing and segregation process in a gas fluidized bed with bi-sized particle mixtures (2 mm in diameter for jetsam particles and 1 mm for flotsam particles with 50% volume fraction for each type of particles) at different densities has been studied using a numerical model by coupling Discrete Element Method (DEM) for the solid phase with Computational Fluid Dynamics (CFD) for the gas phase. It is shown that inverse segregation happens with jetsam particles sitting above flotsam particles by either increasing the density of flotsam particles or decreasing the density of jetsam particles. Two sets of density arrangement corresponding to the maximum mixing have been obtained: 2500 kg m^{-3} for jetsam particles with 4000 kg m^{-3} for flotsam particles; and 1500 kg m^{-3} for jetsam particles and 2500 kg m^{-3} for flotsam particles. It demonstrates the density ratio corresponding to the maximum mixing is dependent on the actual particle densities. The maximum mixing state is independent on gas injection velocities. Further work will be focused on the investigation of the underlying mechanisms governing mixing/segregation based on micro-dynamic information. These detailed investigations, together with extra DEM-CFD simulations if necessary, are expected to yield a predictive model that can be reliably used to assist process design, control and optimisation of gas fluidized particle mixtures.

INTRODUCTION

Solid mixing and segregation are complex phenomena in a gas fluidized bed when particles of different size and/or density exist. The words flotsam and jetsam are introduced to describe the solids which occupy, respectively, the top or bottom part of the bed (Rowe et al., 1972). Usually, larger or heavier particles behave as jetsam, and smaller or lighter particles behave as flotsam. While in a fluidised bed with combined size and density difference, the determination of flotsam or jetsam particles is dependent on size and density ratios. For the convenience of discussion, larger sized particles are called jetsam and smaller sized particles are called flotsam in this work. For the same purpose, the segregation with flotsam particles on the top of jetsam particles is called normal segregation, while the segregation with jetsam particles on the top of flotsam particles is called inverse segregation.

Despite being an intensive research area, because of so many pertinent factors, such as size ratio, density ratio, operation velocity, bed aspect ratio and even gas distributor design, there are no general design rules or predictive models that can reliably predict the performance. The lack of particle scale information prevents a better understanding of the underlying mechanism governing mixing/segregation process.

CFD-DEM modelling can generate detailed particle scale information, such as particle trajectories, transient forces between particles, and between particle and fluid. Analysis based on such micro-dynamic information provides a better understanding of the underlying mechanics governing different gas solid flow behaviour including mixing/segregation of particle mixtures. Since it was introduced by early developers (Tsuji et al., 1993, Hoomans et al., 1996, Xu and Yu, 1997), the CFD-DEM model has received increasing interest over the past years and has been used to study different gas solid flow phenomena in various process industries, as is recently reviewed by Zhu et al. (2007, 2008). Due to the advance of computing facilities, improved parallelisation technology, coupled DEM code with commercial CFD software, CFD-DEM simulation at a process scale with complex geometries has become possible (Chu and Yu, 2008; Dong et al., 2008). Expectedly, CFD-DEM approach will be increasingly used in the future.

In our previous work, a CFD-DEM model has been developed to study mixing/segregation behaviour of a bi-sized system with fixed particle density. The particle sizes are 2 mm in diameter for jetsam particles and 1 mm for flotsam particles, with each type set to 50% in volume fraction. Following model development and validation (Feng et al. 2004, Feng and Yu, 2004), the simulation results have been analysed by focusing either on chaotic behaviour of individual particles (Feng and Yu, 2008) or statistics in terms of force structure and flow structure (Feng and Yu, 2007). Some new insight of mixing/segregation as a function of gas injection velocity has been built up. For example, it is shown that segregation, as a transient process, happens at a certain range of gas injection velocities. The mechanisms can be explained in terms of interaction forces between particles and between particles and fluid. Segregation in the vertical direction takes place when the fluid drag force acting on flotsam is large enough to not only balance its gravity but also break through the suppression of the surrounding jetsam. Both particle-fluid and particle-particle interactions are complicated, varying spatially and temporally. Mixing and segregation, fluidisation and de-fluidisation largely represent the complex dynamic balance of these forces either locally or globally.

These findings inspire our interest in exploring whether it is possible to find a way to predict the maximum mixing or minimum segregation through reducing the density of jetsam particles or increasing the density of flotsam particles so that the two types of particles possess a similar minimum fluidisation velocity. The concept was tested using a CFD-DEM model and proved that the relationship is not straight forward. Many CFD-DEM simulations at different size ratios, density ratios and gas injection velocities are required to build up a predictive model that can reliably predict the phenomena.

This paper presents initial work towards the predictive model for predicting the maximum mixing with a proper combination of size and density ratios. Based on the same bed geometry and particle sizes as used before (Feng et al., 2004), the transition from normal segregation to inverse segregation has been studied by either increasing the density of flotsam particles or reducing the density of jetsam particles. The density differences corresponding to maximum mixing are obtained. Moreover, the effect of gas injection velocity is investigated.

MODEL DESCRIPTION

The simulation is based upon a CFD-DEM model developed at the University of New South Wales, the details of the modeling approach can be found elsewhere (Feng et al., 2004, Feng and Yu, 2004). For brevity, only the key features of the present model are described as below.

The solid phase is treated as a discrete phase that is described by a conventional Discrete Element Method (DEM). The translational and rotational motions of a particle at any time, t, in the bed are determined by Newton's second law of motion. These can be written as:

$$m_i \frac{d\mathbf{v}_i}{dt} = \mathbf{f}_{f,i} + \sum_{j=1}^{k_i} (\mathbf{f}_{c,ij} + \mathbf{f}_{d,ij}) + \mathbf{f}_{g,i} \quad (1)$$

and

$$I_i \frac{d\omega_i}{dt} = \sum_{j=1}^{k_i} \mathbf{T}_{ij} \quad (2)$$

where m_i, I_i, k_i, $\mathbf{v_i}$ and $\boldsymbol{\omega}_i$ are, respectively, the mass, moment of inertia, number of contacting particles, translational and rotational velocities of a particle i; $\mathbf{f}_{f,i}$ and $\mathbf{f}_{g,i}$ are fluid drag force and gravitational force respectively. $\mathbf{f}_{c,ij}$, $\mathbf{f}_{d,ij}$ and $\mathbf{T}_{i,j}$ are the contact force, viscous contact damping force and torque between particles i and j. These inter-particle forces and torques are summed over the k_i particles in contact with particle i.

The contact force between particle-particle and particle-wall is calculated based on the soft-particle method. The particle-fluid interaction force is calculated according to the correlations by Di Felice (1994), recommended by Xu and Yu (1997).

The gas phase is treated as a continuous phase and modelled in a way very similar to the one widely used in the conventional two fluid model (Gidaspow, 1994). Thus, the governing equations are the conservation of mass and momentum in terms of the local mean variables over a computational cell, given by

$$\frac{\partial \varepsilon}{\partial t} + \nabla \cdot (\varepsilon \mathbf{u}) = 0 \quad (3)$$

and

$$\frac{\partial(\rho_f \varepsilon \mathbf{u})}{\partial t} + \nabla \cdot (\rho_f \varepsilon \mathbf{uu}) = -\nabla P - \frac{\sum_{i=1}^{k_c} \mathbf{f}_{f,i}}{\Delta V} + \nabla \cdot (\varepsilon \boldsymbol{\tau}) + \rho_f \varepsilon \mathbf{g} \quad (4)$$

where $\mathbf{u}$ and P respectively are, the fluid velocity and pressure; $\boldsymbol{\tau}$, ε and ΔV are the fluid viscous stress tensor, porosity and volume of a computational cell.

SIMULATION CONDITIONS

The simulation parameters are listed in Table 1, which, except for the particle densities, are the same as used in our previous work (Feng et al., 2004). A few trial runs were conducted to select appropriate gas injection velocities and particle densities. This paper discusses results from 17 runs with the simulation parameters listed in Table 2. The gas injection velocity is set to 1.0 m s^{-1} for the cases with increasing flotsam particle density and 0.8 m s^{-1} for the cases with reducing jetsam particle density. The density ranges ensure the solid flow spans from normal segregation to inverse segregation. Extra runs at other gas injection velocities are conducted for the case when the density of flotsam particles is 4000 kg m^{-3} to check whether the corresponding good mixing state is affected by gas injection velocities.

Solid phase		
Young's modulus (Nm^{-2})		1.0×10^7
Poisson ratio (Nm^{-1})		0.33
Friction coefficient (-)		0.33
Damping coefficient (-)		0.3
Particle diameter (m)	Flotsam	0.001
	Jetsam	0.002
Particle numbers (-)	Flotsam	22,223
	Jetsam	2,777
Gas phase		
Viscosity (kgm^{-1}s^{-1})		1.8×10^{-5}
Density (kg m^{-3})		1.205
Bed height (m)		0.26
Bed width (m)		0.065
Bed thickness (m)		0.0081
Cell width (m)		0.005
Cell height (m)		0.005

Table 1 Parameters used for binary-sized systems

Particle density (kg m^{-3})		Gas injection velocity (m s^{-1})
2 mm particle size (jetsam)	1 mm particle size (flotsam)	
2500	2500	1.0
2500	3000	1.0
2500	3500	1.0
2500	4000	0.7, 0.8, 1.0, 1.25
2500	4500	1.0
2500	5000	1.0
2500	5500	1.0
2500	6000	1.0
2500	6500	1.0
2500	2500	0.8
2000	2500	0.8
1500	2500	0.8
1000	2500	0.8
500	2500	0.8

Table 2 Particle densities and gas injection velocities for different CFD-DEM simulations

RESULTS AND DISCUSSION

Solid flow patterns

Figure 1 shows a normal segregation process with flotsam particles residing above jetsam particles when the gas injection velocity is 1.0 m s^{-1} and the density of flotsam and jetsam particles are 2500 kg m^{-3}. This process has been detailed in previous publications (Feng et al., 2004, Feng and Yu, 2007). This Figure is replotted here for comparison purpose. Note that for better visualization, only particles whose centre points are between $1.5x10^{-3}$ m and $2.5x10^{-3}$ m in the thickness direction are presented. This treatment applies to all other figures illustrating flow patterns.

As shown in Figure 1, once gas is introduced into the bed, segregation appears with jetsam aggregated at the bottom layer gradually. Finally, two layers can be identified. The top layer, rich in flotsam, is in fluidised state, and the bottom layer, rich in jetsam, is in de-fluidised state.

At the same gas injection velocity of 1.0 m s^{-1}, when the density of flotsam particles is 6500 kg m^{-3}, inverse segregation occurs with jetsam particles sitting above flotsam particles. The snapshots corresponding to inverse segregation are shown in Figure 2. Following the inverse segregation, the intensity of fluidisation reduces, and eventually leads to a de-fluidised state. The minimum fluidisation velocity is 1.05 m s^{-1} for jetsam particles and 1.08 m s^{-1} for flotsam particles, which explains why the solid flow is not vigorous in this simulation.

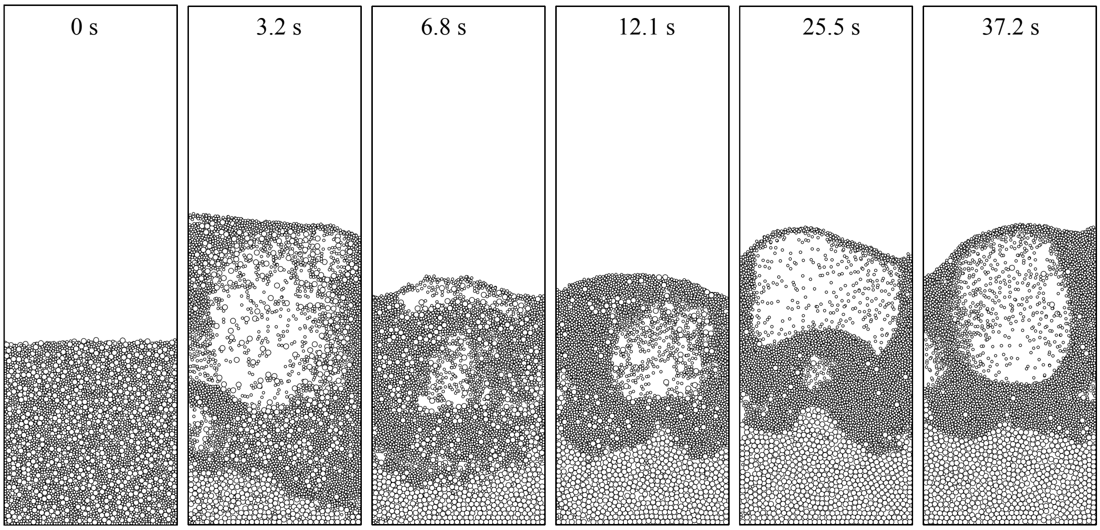

Figure 1: Solid configuration at different times showing normal segregation process with flotsam particles residing on the top of jetsam particles when the gas injection velocity is 1.0 m s^{-1} and the densities of both flotsam and jetsam particles are 2500 kg m^{-3} (Feng and Yu, 2007).

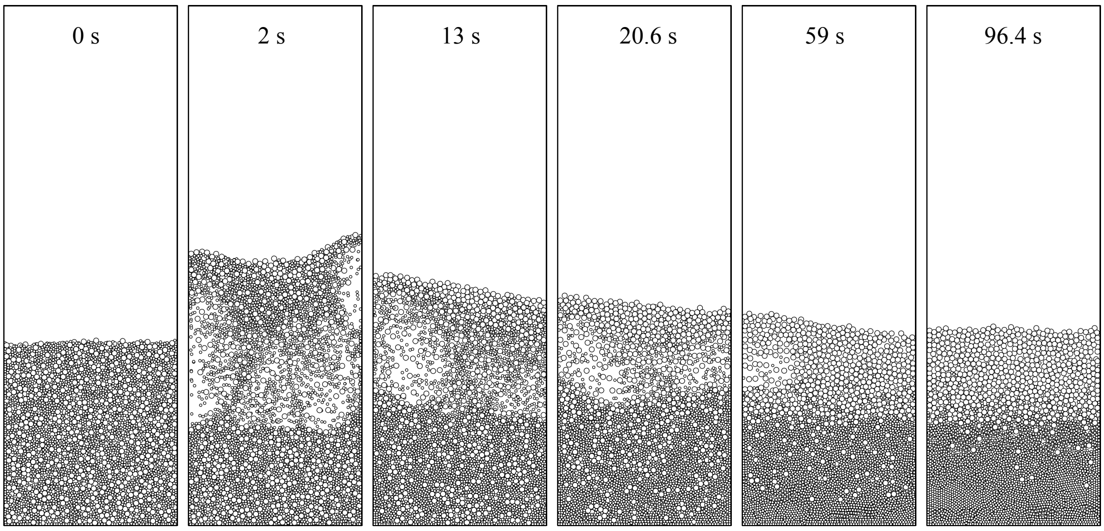

Figure 2: Solid configuration at different times showing inverse segregation process with jetsam particles residing on the top of flotsam particles when the gas injection velocity is 1.0 m s^{-1} and the densities of flotsam and jetsam particles are respectively 6500 and 2500 kg m^{-3}.

Between normal segregation and inverse segregation, there must be a stage corresponding to minimum segregation or maximum mixing. Figure 3 shows the transition from normal segregation to inverse segregation at their dynamically stable state when the density of flotsam particles is increased while the density of jetsam particles is fixed to 2500 kg m^{-3}. The maximum mixing happens when the density of flotsam particles is 4000 kg m^{-3}, at which, almost perfect mixing was observed (Figure 3c). Reasonable mixing occurs in a wide range of flotsam densities, roughly between 3000 and 5000 kg m^{-3}.

Figure 4 shows the transition from normal segregation to inverse segregation at gas injection velocity 0.8 m s^{-1} when the density of flotsam particles increases while the density of jetsam particles is fixed to 2500 kg m^{-3}. A well mixed solid flow is achieved when the density of jetsam particles is about 1500 kg m^{-3}.

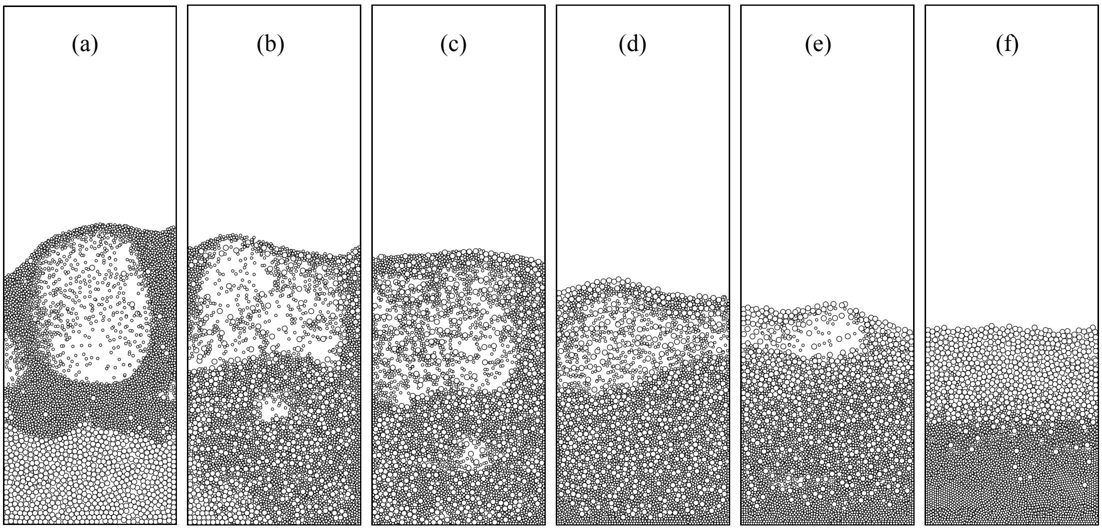

Figure 3: Solid configurations at dynamically stable states showing the transition from normal segregation to inverse segregation at the gas injection velocity 1.0 m s^{-1} when the density of flotsam particles is: (a) 2500, (b) 3000, (c) 4000, (d) 5000, (e) 6000, (f) 6500 kg m^{-3}.

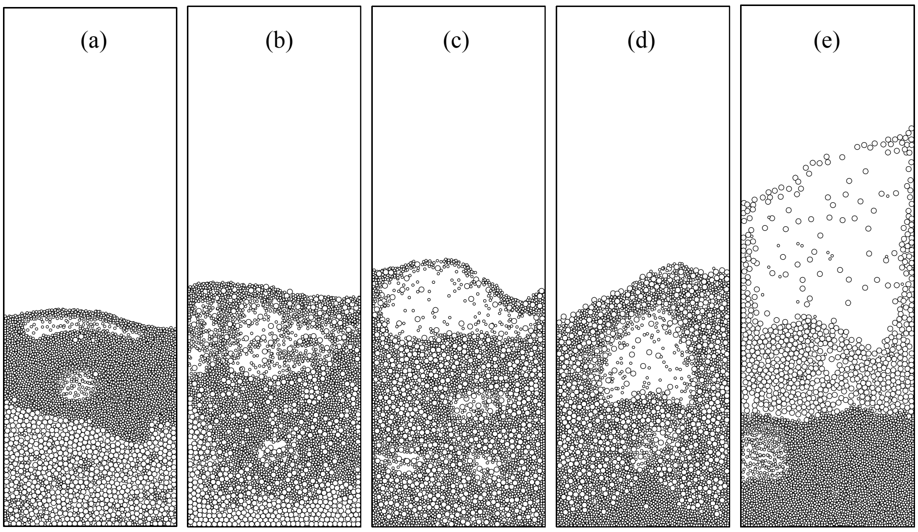

Figure 4: Solid configurations at dynamically stable states showing the transition from normal segregation to inverse segregation at the gas injection velocity 0.8 m s^{-1} when the density of jetsam particles is: (a) 2500, (b) 2000, (c) 1500, (d) 1000, (e) 500 kg m^{-3}.

Mixing/segregation kinetics and determination of maximum mixing state

The kinetics of mixing/segregation process is often quantified by mixing index in which many forms have been used in the past as reviewed by Fan et al (1970) and more recently Poux et al (1991). Lacey mixing index was used in our previous work (Feng et al., 2004), while its value is affected on sample size. Here, the mixing kinetics is simply expressed by vertical mean positions for each type of particles.

Figure 5a shows the mean position of each type of particles when the density of flotsam particles is 2500 kg m^{-3}. Corresponding to the normal segregation shown at Figure 1, the mean position increases for flotsam particles and decreases for jetsam particles. The time to reach a dynamically stable state is about 20 seconds that is consistent with the previous study expressed using Lacey mixing index (Feng et al., 2004). Figure 5b shows the mean position corresponding to Figure 3c where the mean positions of two types of particles are very similar. Figure 5c shows the particle mean position of an inverse segregation corresponding to case shown at Figure 2. It takes about 100 seconds for the particles to rearrange to a dynamically stable state. The mean value over time at their respective dynamically stable state is calculated and plotted in Figure 6. With the increase of the density of flotsam particles, the mean value decreases for flotsam particles and increases for jetsam particles. The intersection point of the two lines gives the density of flotsam particles corresponding to maximum mixing which is consistent with observation shown in Figure 3c.

Figures 7&8 plot the data in the same way as Figures 5&6, but for the cases with decreased densities of jetsam particles while the gas injection velocity is set to 0.8 ms^{-1}. Consistent with observation in Figure 4c, the maximum mixing occurs when the jetsam particles' density is 1500 kg m^{-3}.

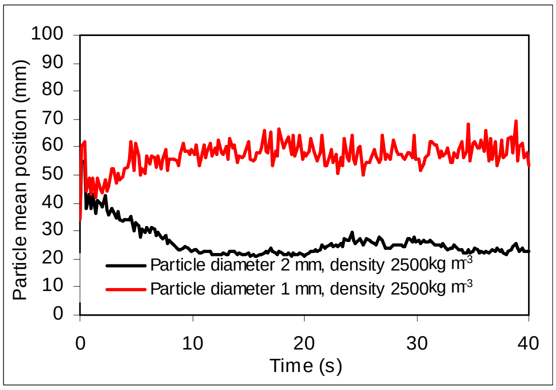

(a)

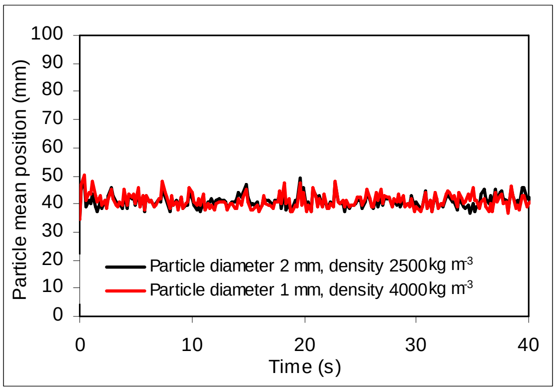

(b)

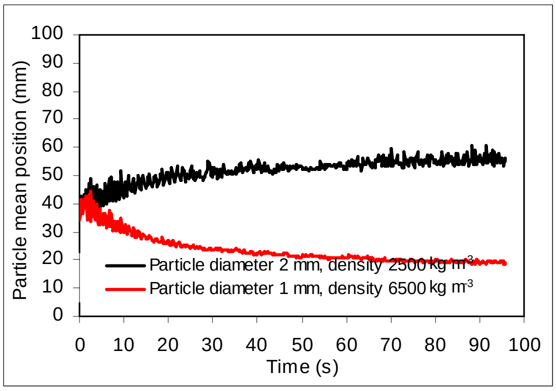

(c)

Figure 5: Variation of particle mean vertical position with time at different densities of small size particles when the gas injection velocity is 1.0 m s^{-1}.

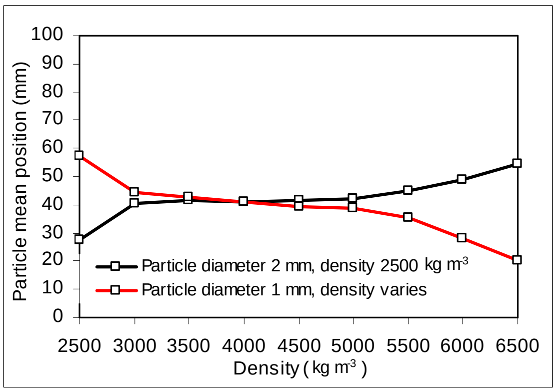

Figure 6: Vertical mean position of each type particles at dynamically stable state at different densities of small size particles when the gas injection velocity is 1.0 m s^{-1}.

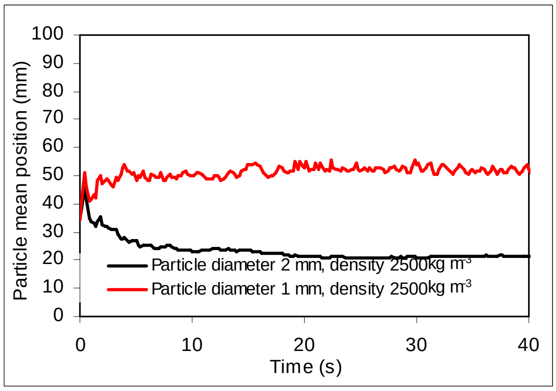

(a)

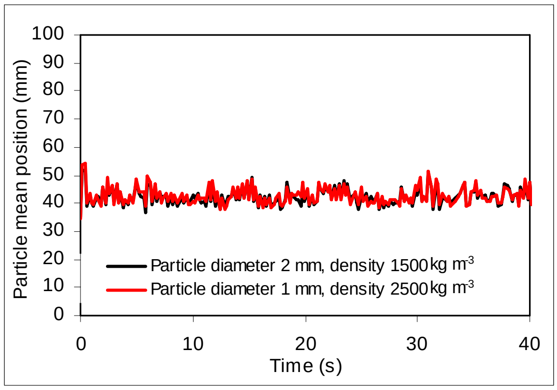

(b)

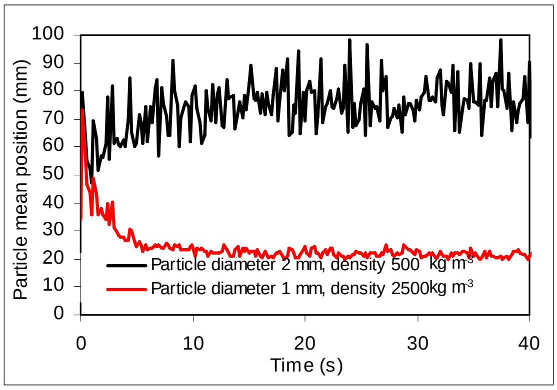

(c)

Figure 7: Variation of particle mean vertical position with time at different densities of large size particles when the gas injection velocity is 0.8 m s^{-1}.

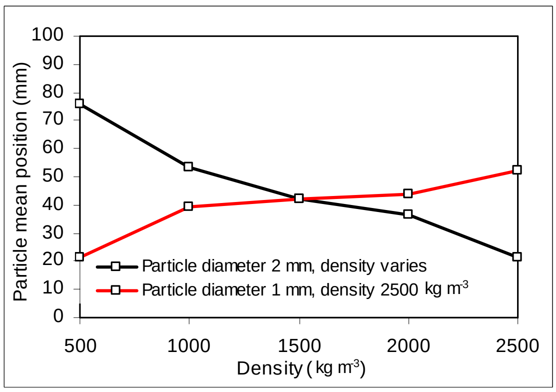

Figure 8: Vertical mean position of each type particles at dynamically stable state at different densities of large size particles when the gas injection velocity is 0.8 m s^{-1}.

Effect of gas injection velocity

The above study is based on one velocity. It is interesting to know whether the maximum mixing state is sensitive to gas injection velocities or not. To answer this question, three more simulations have been conducted at gas injection velocities 0.7, 0.8 and 1.25 m s^{-1} when the density of flotsam particles is 4000 kg m^{-3} which demonstrated a good mixing at gas injection velocity of 1.0 m s^{-1} (Figure 3c).

When the gas injection velocity is 0.7 m s^{-1}, the particles undergo a little rearrangement to form clusters of different types of particles and then stay as a fixed bed (Figure 9a). Their mean values are constant (Figure 10a). Figure 9b displays the solid particles when the gas injection velocity is 0.8 m s^{-1}. The particles are not uniformly distributed. Each type of particle aggregates together to form some local clusters. Dynamic investigation of the flow patterns shows that the clusters of each types of particles recirculate in the bed. This is reflected by plotting their averaged mean positions as shown in Figure 10b. When the velocity is high enough, strong fluidization leads to good mixing (Figure 9c and 10c). In general, good mixing happens at all velocities investigated.

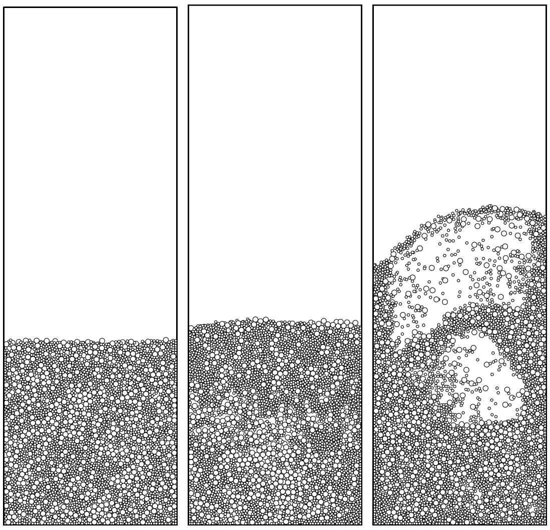

(a) **(b)** **(c)**

Figure 9: Solid configurations at dynamically stable state when the density of jetsam particles is 2500 kg m^{-3} and the density of flotsam particles is 4000 kg m^{-3} at gas injection velocities: (a) 0.7 m s^{-1}, (b) 0.8 m s^{-1}, (c) 1.25 m s^{-1}.

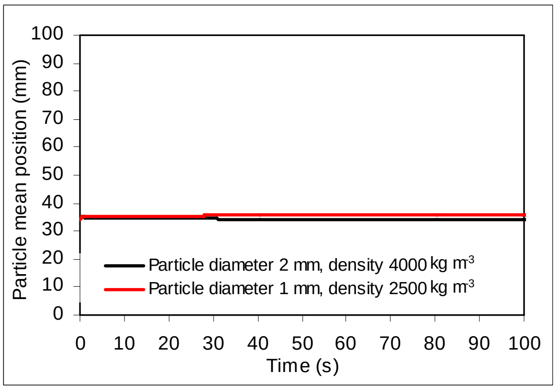

(a)

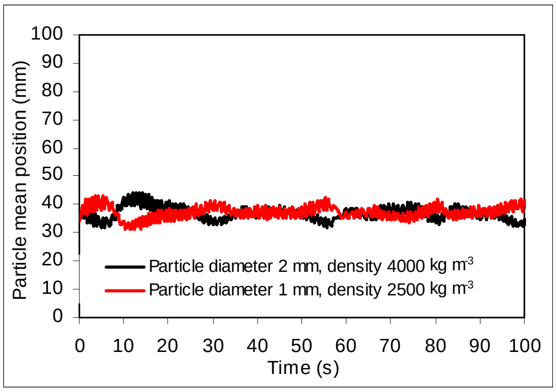

(b)

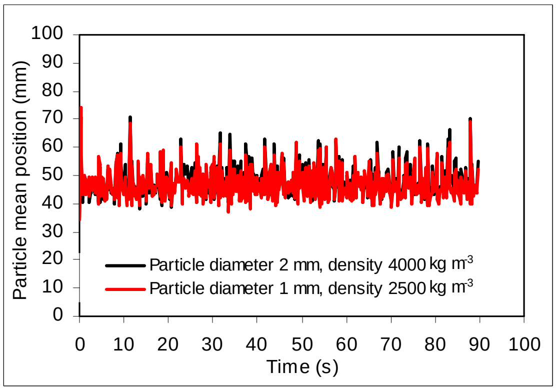

(c)

Figure 10: Variation of particle mean position in vertical direction at different gas injection velocities: (a) 0.7 m s^{-1}, (b) 0.8 m s^{-1}, (c) 1.25 m s^{-1}.

CONCLUSIONS

CFD-DEM approach has been used to study the mixing/segregation behaviour of particle mixtures in a gas fluidized bed. At a fixed size ratio (2 mm in diameter for jetsam particles and 1 mm for flotsam particles), inverse segregation happens with jetsam particles sitting above flotsam particles by either reducing the density of jetsam particles or increasing the density of flotsam particles. The maximum mixing can be achieved at an appropriate density difference between flotsam and jetsam particles which is dependent on the actually particle densities. The maximum mixing is independent of the gas injection velocities.

Present discussions of CFD-DEM results based on solid flow patterns and mixing/segregation kinetics are very preliminary. However, it demonstrates that mixing and segregation is a complex process which prevents it being predicted by a simple design rules. In the future, micro-dynamic analysis will be conducted to investigate the underlying mechanisms. These detailed investigations, together with extra CFD-DEM simulations if necessary, are expected to lead to a predictive model that can be used to assist process design, control and optimisation of gas fluidized particle mixtures.

ACKNOWLEDGEMENT

The authors thank for the advanced computing facilities provided by IVEC (Interactive Virtual Environments Centre).

REFERENCES

CHU, K.W. and Yu, A.B., (2008), Numerical simulation of complex particle-fluid flows, Powder Technology, 179, 104-114.

DI FELICE, R., (1994), The voidage function for fluid-particle interaction systems, International Journal of Multiphase Flow, 20, 153-159.

DONG, K.J., Guo, B.Y., Chu, K.W., Yu, A.B., Brake, I., (2008), Simulation of liquid-solid flow in a coal distributor, Minerals Engineering, 21, 789-796

FENG, Y.Q., Yu, A.B., (2004), Assessment of model formulations in the discrete particle simulation of gas-solid flow, Industrial and Engineering Chemistry Research, 43, 8378-8390.

FENG, Y.Q., Xu, B.H., Zhang, S. J., Yu, A.B., Zulli, P., (2004), Discrete particle simulation of gas fluidization of particle mixtures, AIChE Journal 50, 1713-1728.

FENG, Y.Q., Yu, A.B., Microdynamic modelling and analysis of the fluidisation and segregation of binary mixtures of particles, Chemical Engineering Science, 2007, 62, 256-268.

FENG, Y.Q., Yu, A.B., An analysis of the chaotic motion of particles of different sizes in a gas fluidized bed, (2008), Particuology, 6 (6), 549-556.

FAN, L.T., S.J. Chen & C.A. Watson, "Solid mixing," Industrial and Engineering Chemistry, 62, 53-69 (1970).

GIDASPOW, D., (1994), Multiphase Flow and Fluidization, Academic Press, San Diego.

HOOMANS, B.P.B.; Kuipers, J.A.M.; Briels, W. J.; Van Swaaij, W.P.M., (1996), Discrete particle simulation of bubble and slug formation in a two-dimensional gas-fluidised bed: a hard –sphere approach, Chemical Engineering Science, 51, 99-118.

POUX, M, P. Fayolle, J. Bertrand, D. Bridoux, and J. Bousquet, (1991), Powder mixing: some practicle rules applied to agitated systems, Powder Technology, 68, 213-234.

ROWE, P. N., Nienow, A. W. and Agbim, A. J., (1972), The mechanisms by which particles segregate in gas fluidised beds – binary systems of near-spherical particles, Trans. Insti. Chem. Engrs., 50, 310-323.

TSUJI, Y., Kawaguchi, T., Tanaka, T. Discrete particle simulation of two-dimensional fluidised bed, (1993), Powder Technology, 77, 79-87.

XU, B.H., Yu, A.B., (1997), Numerical simulation of the gas solid flow in a fluidized bed by combining discrete particle method with computational fluid dynamics, Chemical Engineering Science, 52, 2785-2809.

ZHU, H.P., Zhou, Z.Y., Yang, R.Y. and Yu, A.B., (2007), Discrete particle simulation of particulate systems: Theoretical developments, Chemical Engineering Science, 62, 3378-3396.

ZHU, H.P., Zhou, Z.Y., Yang, R.Y., Yu, A.B., (2008), Discrete particle simulation of particulate systems: A review of major applications and findings, Chemical Engineering Science, 63, 5728-5770.